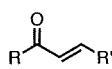


Table 7. Inhibition Constants of Chalcone and Chalcone-Like Derivatives on Ligand Binding to A β (1–42) Aggregates



Compd.	R	R'	K _i (nM) ^{a)}
17	4-Aminophenyl	4-Iodophenyl	248 ± 56
18	4-Methylaminophenyl	4-Iodophenyl	23.9 ± 3.6
19	4-Dimethylaminophenyl	4-Iodophenyl	13.3 ± 1.9
20	5-Iodo-2-thienyl	4-Aminophenyl	121 ± 40
21	5-Iodo-2-thienyl	4-Methylaminophenyl	14.1 ± 0.6
22	5-Iodo-2-thienyl	4-Dimethylaminophenyl	3.9 ± 0.4
23	4-Aminophenyl	5-Bromo-2-thienyl	476 ± 48
24	4-Methylaminophenyl	5-Bromo-2-thienyl	198 ± 49
25	4-Dimethylaminophenyl	5-Bromo-2-thienyl	106 ± 7.1
26	4-Iodophenyl	Phenyl	151 ± 16
27	4-Iodophenyl	2-Furanyl	908 ± 212
28	4-Iodophenyl	3-Furanyl	125 ± 9.2
29	4-Iodophenyl	2-Thienyl	102 ± 16
30	4-Iodophenyl	3-Thienyl	93 ± 11
31	4-Iodophenyl	2-Imidazolyl	797 ± 316
32	4-Iodophenyl	2-Thiazolyl	>10000
33	4-Iodophenyl	5-Dimethylamino-2-furanyl	1132 ± 344
34	4-Iodophenyl	5-Dimethylamino-2-thienyl	113 ± 10
35	5-Iodo-2-thienyl	5-Dimethylamino-2-thienyl	137 ± 3.4
36	5-Iodo-2-thienyl	5-Dimethylamino-2-furanyl	1608 ± 85
37	5-Bromo-2-furanyl	4-Dimethylaminophenyl	126 ± 13
38	5-Bromo-2-furanyl	5-Dimethylamino-2-thienyl	2648 ± 222
39	5-Bromo-2-furanyl	5-Dimethylamino-2-furanyl	>10000
CR	—	—	>10000
ThT	—	—	>10000
AIC ^{b)}	4-Iodophenyl	4-Aminophenyl	105 ± 12
IMC ^{c)}	4-Iodophenyl	4-Methylaminophenyl	6.3 ± 1.6
DMIC ^{d)}	4-Iodophenyl	4-Dimethylaminophenyl	2.9 ± 0.3

a) Values are means ± S.E. of 3–6 independent experiments. b) 4-Amino-4'-iodo-chalcone. c) 4'-Iodo-4-methylamino-chalcone. d) 4-Dimethylamino-4'-iodo-chalcone. b, c, d) Our unpublished data.⁴²⁾

cone-like compounds had high binding affinity for A β (1–42) aggregates in the order of *N,N*-dimethylated derivatives (19, 20) > *N*-monomethylated derivatives (18, 37) > primary amino derivatives (17, 35) when comparing similar core structures. Compounds 17, 18, and 19 with a substituted group at the 4'-position and iodine at the 4-position displayed higher K_i values (lower binding affinities) as compared with compounds 4-amino-4'-iodo-chalcone (AIC), 4'-iodo-4-methylamino-chalcone (IMC), and DMIC, which have a substituted group and iodine at the inverse position against compounds 17, 18, and 19. The K_i values of 36, 38, and 39 with a thienyl group at the R-position and phenyl group at the R'-position were higher than those of 35, 37, and 20 with a phenyl group at the R-position and thienyl group at the R'-position, indicating that the binding affinities depend on the combination of heterocycles introduced at the R- and R'-positions and not on the position of the substituted group or iodine (bromine) group. When comparing the K_i values of heterocyclic compounds with the same substituted group, the binding affinities increased in the order of phenyl > thienyl > furanyl at the R-position and phenyl = thienyl > furanyl at the R'-position. The K_i values of compounds without the substituted group on the ring at the R'-position (21–27) were varied by altering the type of heterocycle. Furthermore, to obtain information on the binding site of the new chalcone-like compounds, inhibition studies were carried out using CR and ThT, which are well-known proto-

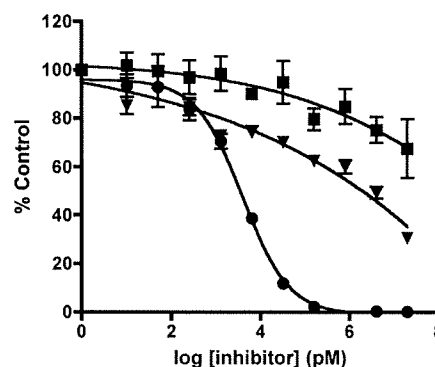
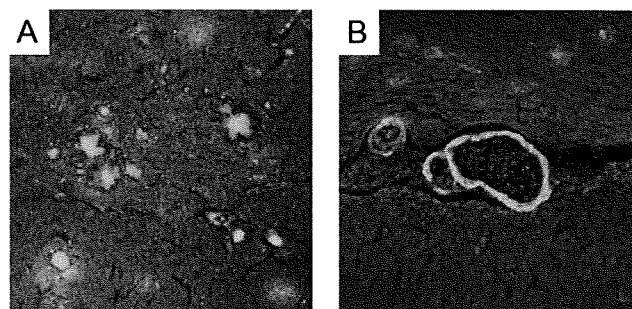
Fig. 10. Competition Curves of [¹²⁵I]DMIC against Compound 20 (Closed Circle), CR (Closed Square), and ThT (Closed Triangle)

Fig. 11. Neuropathological Fluorescent Staining of Compound 20 on AD Model Mouse Brain Sections

(A) Compound 20 intensely stained A β plaques. (B) Clear staining of cerebrovascular amyloids was also observed.

Table 8. Brain Uptake of Radioactivity after Intravenous Injection of [¹²⁵I]20 in Mice^{a)}

	Time after injection (min)			
	2	10	30	60
	2.46	0.75	0.31	0.21
	(0.30)	(0.31)	(0.04)	(0.02)

a) Expressed as % injected dose per gram. Each value represents the mean ± S.D. for five mice at each interval.

types of A β imaging probes. While compound 20 competed for [¹²⁵I]DMIC binding to A β (1–42) aggregates, CR and ThT did not exhibit a dose-dependent decrease in the specific binding of [¹²⁵I]DMIC (Fig. 10).

To confirm the binding affinity to A β plaques in the AD brain, fluorescent staining of AD model mouse brain sections was carried out using the fluorescence of compound 20 (Fig. 11). Compound 20 intensely stained A β plaques in the brain sections. Also, clear staining of cerebrovascular amyloid was observed. This result suggests that compound 20 should detect A β plaques in AD brains.

The radioiodinated compound [¹²⁵I]20 was evaluated for its *in vivo* biodistribution in normal mice (Table 8). Initial brain uptake of [¹²⁵I]20 was 2.46% of injected dose/g at 2 min after intravenous injection, whereas the radioactivity accumulated in the brain was rapidly eliminated (0.21% of injected dose/g, 60 min postinjection), indicating highly desirable properties for an A β imaging agent. Taken together, the data suggest that [¹²⁵I]20 should be further investigated as a potentially useful β -amyloid imaging probe.

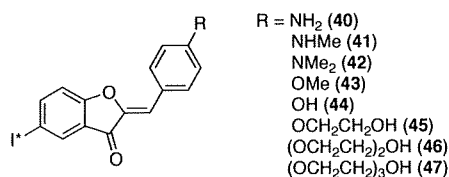
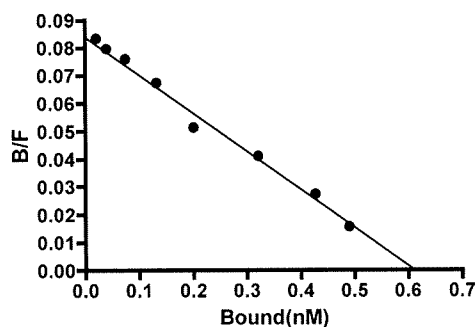


Fig. 12. Chemical Structure of Aurone Derivatives

Fig. 13. Scatchard Plots of [¹²⁵I]40 Binding to Aβ(1—42) Aggregates
 High binding affinity with a K_d value in a nanomolar range was obtained.

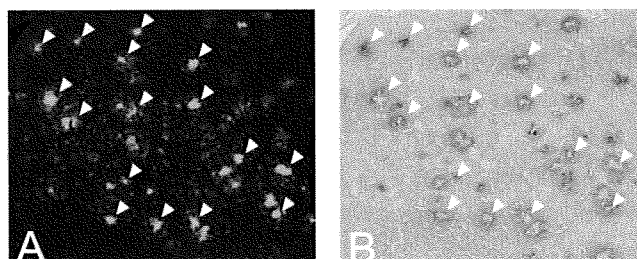
Aurone-Based Aβ Imaging Probes To explore more useful candidates for core structures of Aβ imaging probes, we selected one of the flavonoids, aurone, as a new core structure. First, we synthesized a series of aurone derivatives, which possess a radioiodine at the 5-position and a nucleophilic group (NH₂, NHMe, NMe₂) at the 4'-position, and evaluated their biological activities as *in vivo* Aβ imaging probes (Fig. 12).⁴⁷⁾ To evaluate the binding affinity of aurone derivatives to Aβ aggregates, a saturation assay with [¹²⁵I]40 was carried out using Aβ(1—42) aggregates. When the saturation bindings of [¹²⁵I]40 were transformed to Scatchard plots, they showed linear plots, indicating that aurone derivatives have one binding site on Aβ aggregates (Fig. 13). [¹²⁵I]40 displayed excellent binding affinity for Aβ(1—42) aggregates with a K_d value of 7.9 ± 1.3 nM. Binding affinities of nonradioactive aurones (**40**, **41**, **42**) were also evaluated with inhibition studies against [¹²⁵I]40 binding on Aβ(1—42) aggregates (Table 9). The K_i values estimated for **40**, **41**, and **42** were 2.7, 1.2, and 6.8 nM for Aβ(1—42) aggregates, respectively. These K_i values suggested that the new series of aurones had excellent binding affinity for Aβ(1—42) aggregates and showed considerable tolerance for structural modification. The K_i values of the radioiodinated aurones reported previously were lower than those of the radioiodinated flavones, indicating that the radioiodinated aurones have higher binding affinities to Aβ plaques than those of the corresponding radioiodinated flavones and chalcones.

To confirm the binding affinity of aurone derivatives to Aβ plaques in the brain, neuropathologic fluorescent staining with compound **42** was carried out using double-transgenic Alzheimer's mouse brain sections (Fig. 14). Many Aβ plaque deposits were clearly stained with compound **42**, as reflected by the high binding affinity to Aβ aggregates in *in vitro* competition assays. The compound clearly stained not only core plaques, but also typical senile plaques. The labeling pattern was consistent with that observed with immunohistochemical labeling with an antibody specific for Aβ, indicating that aurone derivatives show specific binding to Aβ plaques. Thus

Table 9. Inhibition Constants of Aurone Derivatives on Ligand Binding to Aβ(1—42) Aggregates

Compound	K_i (nM) ^{a)}
40	2.69 ± 0.16
41	1.24 ± 0.11
42	6.82 ± 0.48

a) Values are means \pm S.E. of three independent experiments.

Fig. 14. Neuropathological Staining of Compound **42** on 5 μm AD Model Mouse Sections from the Cortex

(A) Many Aβ plaques are clearly stained with compound **42**. (B) The same sections were immunostained using an antibody against Aβ.

Table 10. Biodistribution of Radioactivity after Intravenous Injection of [¹²⁵I]40, [¹²⁵I]41, and [¹²⁵I]42 in Mice^{a)}

Compound	Time after injection (min)			
	2	10	30	60
[¹²⁵ I]40	4.57 (0.27)	1.51 (0.17)	0.49 (0.06)	0.26 (0.03)
[¹²⁵ I]41	3.17 (0.45)	1.22 (0.09)	0.32 (0.02)	0.24 (0.03)
[¹²⁵ I]42	1.89 (0.38)	0.69 (0.21)	0.26 (0.04)	0.11 (0.03)

a) Expressed as % injected dose per gram. Each value represents the mean \pm S.D. for five mice at each interval.

the results suggest that aurone derivatives may be applicable for *in vivo* imaging of Aβ plaques in the brain.

To evaluate the brain uptake of the aurone derivatives, *in vivo* biodistribution studies in normal mice were performed with three radioiodinated aurones ([¹²⁵I]40, [¹²⁵I]41, and [¹²⁵I]42) (Table 10). The aurone derivatives displayed high brain uptake rates ranging from 1.9—4.6% ID/g brain at 2 min postinjection, indicating a level sufficient for Aβ imaging of the brain. In addition, they displayed rapid clearance from the normal brain with 0.49%, 0.32%, and 0.26% ID/g at 30 min postinjection for [¹²⁵I]40, [¹²⁵I]41, and [¹²⁵I]42, respectively. These values were equal to 10.7%, 10.1%, and 13.8% of the initial brain uptake peak for [¹²⁵I]40, [¹²⁵I]41, and [¹²⁵I]42, respectively. We reported that radioiodinated flavones showed high brain uptake (3.2—4.1% ID/g at 2 min postinjection) and good clearance from the brain (0.5—1.9% ID/g at 30 min postinjection). However, the ratios of 2- to 30-min mouse brain uptake of the radioiodinated flavones were 40.0%, 44.6%, and 57.8% for NH₂, NHMe, and NMe₂ derivatives, respectively, which were higher than those of radioiodinated aurones. The result suggests that aurone derivatives do not show high nonspecific binding in the brain *in vivo*. These desirable pharmacokinetics demonstrated by radioiod-

inated aurones are critical to detect $A\beta$ plaques in the AD brain. These biodistribution data suggest that novel radioiodinated aurones may have more suitable *in vivo* pharmacokinetic properties for $A\beta$ imaging in AD brains compared with the radioiodinated flavones and chalcones. However, these aurone derivatives appeared inferior to IMPY in pharmacokinetics, although their high affinity for $A\beta$ plaques is sufficient for imaging *in vivo*. Therefore additional structural changes are essential to improve the properties of aurone derivatives to make them suitable for the imaging of $A\beta$ plaques in the brain.

To develop more promising aurones for SPECT-based imaging of $A\beta$ plaques, we designed a novel series of radioiodinated derivatives with polyethylene glycol (PEG).⁴⁸⁾ PEG is nontoxic, nonimmunogenic, highly soluble in water, and FDA approved, and PEGylation has been used to change the pharmacokinetics of various biologically interesting proteins or peptides, leading to better therapeutics.^{49,50)} Therefore PEGylated aurone derivatives are worthy of further evaluation as novel $A\beta$ imaging probes for SPECT.

We designed and synthesized a novel series of radioiodinated aurone derivatives with not only 1 to 3 units of ethylene glycol at the 4' position, but also other nucleophilic groups ($-OCH_3$ and $-OH$) (Fig. 12) and evaluated their biological potential as probes for imaging $A\beta$ by testing their affinity for $A\beta$ aggregates *in vitro* and their uptake by and clearance from the brain in biodistribution experiments using normal mice.

Our initial screening of the affinity of aurone derivatives (43, 44, 45, 46, 47) was carried out with $A\beta(1-42)$ aggregates, using [¹²⁵I]AAU as the competing radioligand (Table 11). The K_i values estimated for 43, 44, 45, 46, and 47 were 2.9, 1.3, 1.1, 3.4, and 2.6 nM, respectively. These values suggested that the new series of aurone derivatives had binding affinity for $A\beta(1-42)$ aggregates despite their substituted groups. The binding affinity is in the same range as that of aurone derivatives possessing a nucleophilic group (NH_2 , $NHMe$, NMe_2).⁴⁷⁾ These results clearly indicate that aurone derivatives exhibit considerable tolerance to structural modifications. The binding affinity of aurone derivatives is very close to that of known $A\beta$ imaging probes such as SB-13 ($K_i=1.2$ nM),⁵¹⁾ PIB ($K_i=2.8$ nM),⁵²⁾ and IMPY ($K_i=1.4$ nM),⁵¹⁾ indicating that they have sufficient affinity to test clinically.

To confirm the affinity of aurone derivatives for $A\beta$ plaques in the mouse brain, neuropathologic fluorescent staining with 43, 44, 45, 46, and 47 was carried out using double-transgenic Alzheimer's mouse brain sections (Fig. 15). Many $A\beta$ plaque deposits were clearly stained with the derivatives, as reflected by the high binding affinity for $A\beta$ aggregates in *in vitro* competition assays. The labeling pattern was consistent with that observed with ThS. These results suggest that novel aurone derivatives show affinity for $A\beta$ plaques in the mouse brain in addition to having binding affinity for synthetic $A\beta_{42}$ aggregates.

To evaluate brain uptake of the aurone derivatives, biodistribution experiments were performed in normal mice with five radioiodinated aurones ([¹²⁵I]43, [¹²⁵I]44, [¹²⁵I]45, [¹²⁵I]46, and [¹²⁵I]47) (Table 12). Radioactivity after injection of the aurone derivatives penetrated the BBB and showed excellent uptake ranging from 1.7 to 4.5% ID/g brain at 2 min

Table 11. Inhibition Constants of Newly Synthesized Aurone Derivatives for the Binding of Ligands to $A\beta(1-42)$ Aggregates

Compound	K_i (nM) ^{a)}
43	2.89±0.42
44	1.28±0.29
45	1.05±0.06
46	3.36±0.29
47	2.56±0.31

a) Data are the mean±S.E. for two independent measurements done in triplicate.

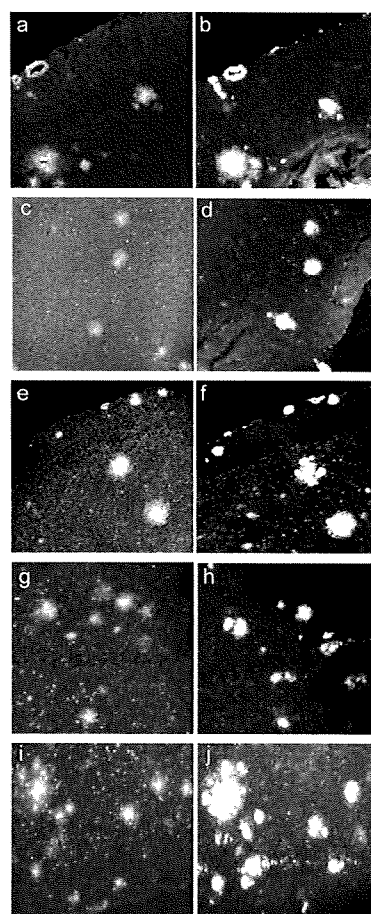


Fig. 15. Neuropathological Staining of 43, 44, 45, 46, and 47 (a, c, e, g, i) in 10 μ m Sections from a Mouse Model of AD

Labeled plaques were confirmed by staining of the adjacent sections with ThS (b, d, f, h, j).

postinjection, a level sufficient for imaging $A\beta$ plaques in the brain. In addition, it displayed good clearance from the normal brain with 0.1–0.4% ID/g at 30 min postinjection. One method to select a ligand with appropriate *in vivo* kinetics is to use $brain_{2\min}/brain_{30\min}$ as an index to compare the washout rate. The five radioiodinated aurone derivatives [¹²⁵I]43, [¹²⁵I]44, [¹²⁵I]45, [¹²⁵I]46, and [¹²⁵I]47 showed $brain_{2\min}/brain_{30\min}$ ratios of 15.4, 8.3, 18.8, 9.7, and 15.6, respectively. [¹²⁵I]45 had the best washout index. Previously reported radioiodinated aurones showed high uptake (1.9–4.6% ID/g at 2 min postinjection) and good clearance from the brain (0.3–0.5% ID/g at 30 min postinjection).⁴⁸⁾ However, the $brain_{2\min}/brain_{30\min}$ ratios of these compounds were 7.3–9.9, lower than that of [¹²⁵I]45, indicating that [¹²⁵I]45 could clear more rapidly from the normal mouse brain than

Table 12. Biodistribution of Radioactivity after Injection of Aurone Derivatives in Mice^{a)}

Tissue	Time after injection (min)			
	2	10	30	60
[¹²⁵ I]43				
Blood	3.16 (0.82)	1.51 (0.23)	0.95 (0.19)	0.70 (0.60)
Liver	6.87 (2.18)	5.16 (0.73)	2.76 (0.40)	1.86 (0.83)
Kidney	7.26 (2.18)	7.00 (1.49)	4.93 (1.52)	2.43 (1.17)
Intestine	1.59 (0.51)	4.70 (1.46)	11.67 (3.56)	9.02 (3.14)
Spleen	1.45 (0.56)	0.74 (0.10)	0.48 (0.10)	0.43 (0.14)
Pancreas	2.83 (0.75)	0.77 (0.17)	0.62 (0.75)	0.16 (0.05)
Heart	3.84 (1.04)	1.06 (0.10)	0.37 (0.09)	0.25 (0.12)
Stomach ^{b)}	0.39 (0.20)	0.89 (0.48)	0.42 (0.13)	0.82 (0.46)
Brain	1.69 (0.43)	0.54 (0.12)	0.11 (0.05)	0.03 (0.02)
[¹²⁵ I]44				
Blood	3.14 (0.39)	2.77 (0.28)	1.75 (0.38)	0.87 (0.28)
Liver	6.05 (1.49)	6.63 (1.08)	4.23 (0.63)	4.45 (3.14)
Kidney	11.08 (2.96)	11.22 (2.26)	5.82 (1.11)	2.43 (1.04)
Intestine	2.11 (0.75)	6.12 (0.83)	12.67 (2.13)	14.87 (5.42)
Spleen	2.18 (0.48)	1.36 (0.83)	0.69 (0.14)	0.42 (0.02)
Pancreas	5.28 (0.99)	2.65 (0.64)	0.92 (0.19)	0.36 (0.09)
Heart	6.23 (0.63)	2.57 (0.41)	0.98 (0.14)	0.42 (0.14)
Stomach ^{b)}	0.93 (0.28)	1.46 (0.23)	1.22 (0.72)	1.89 (1.01)
Brain	3.07 (0.39)	1.48 (0.19)	0.37 (0.07)	0.14 (0.12)
[¹²⁵ I]45				
Blood	4.97 (0.96)	3.88 (1.09)	2.38 (0.85)	1.24 (0.35)
Liver	13.4 (3.20)	13.3 (2.59)	7.60 (1.95)	5.27 (0.64)
Kidney	11.3 (1.23)	10.8 (2.58)	6.09 (2.43)	2.50 (1.30)
Intestine	2.78 (0.42)	7.83 (2.22)	17.82 (3.58)	20.93 (4.46)
Spleen	2.72 (0.28)	1.02 (0.22)	0.50 (0.13)	0.21 (0.09)
Pancreas	6.38 (0.63)	1.61 (0.61)	0.59 (0.21)	0.29 (0.15)
Heart	6.30 (0.65)	2.30 (0.46)	0.83 (0.15)	0.72 (0.58)
Stomach ^{b)}	1.88 (0.41)	3.23 (2.58)	5.15 (4.43)	1.45 (0.78)
Brain	4.51 (0.25)	1.48 (0.28)	0.24 (0.03)	0.09 (0.04)
[¹²⁵ I]46				
Blood	3.61 (0.74)	5.18 (2.54)	1.11 (0.73)	0.68 (0.45)
Liver	12.5 (3.21)	11.6 (1.75)	9.31 (2.66)	7.12 (4.05)
Kidney	12.0 (0.99)	10.3 (1.17)	5.75 (1.53)	2.55 (1.12)
Intestine	2.35 (1.33)	8.18 (2.32)	19.7 (7.86)	26.38 (5.95)
Spleen	2.26 (0.53)	1.56 (0.45)	0.78 (0.26)	0.45 (0.21)
Pancreas	5.67 (2.72)	2.24 (0.68)	1.40 (0.44)	0.39 (0.29)
Heart	6.04 (0.38)	2.77 (0.94)	1.21 (0.66)	0.66 (0.57)
Stomach ^{b)}	1.71 (0.38)	5.65 (6.63)	5.00 (2.83)	6.58 (4.59)
Brain	3.69 (0.22)	1.53 (0.31)	0.38 (0.05)	0.16 (0.03)
[¹²⁵ I]47				
Blood	2.98 (0.64)	4.62 (2.17)	0.83 (0.64)	0.51 (0.31)
Liver	12.95 (3.43)	11.20 (1.51)	8.34 (1.98)	7.70 (3.93)
Kidney	11.58 (1.13)	9.66 (2.28)	5.84 (1.79)	2.41 (1.22)
Intestine	2.52 (0.39)	7.50 (4.85)	17.95 (7.53)	22.64 (5.89)
Spleen	2.26 (0.65)	1.40 (0.23)	0.84 (0.23)	0.56 (0.24)
Pancreas	5.51 (0.59)	1.84 (0.44)	0.87 (0.37)	0.79 (0.70)
Heart	5.67 (1.02)	2.24 (0.56)	1.40 (0.49)	0.39 (0.68)
Stomach ^{b)}	3.29 (1.47)	4.73 (5.14)	7.45 (4.62)	7.61 (5.20)
Brain	2.81 (0.19)	2.32 (0.21)	0.18 (0.06)	0.08 (0.04)

a) Each value represents the mean ± S.D. for 4–5 animals. b) Expressed as % injected dose per organ.

aurones with amino groups. It has been reported that [¹²³I]IMPY enters the brain rapidly (2.88% ID at 2 min postinjection) and was cleared from the normal brain (0.26% ID at 30 min postinjection), indicating the brain_{2 min}/brain_{30 min} ratio to be 11.1.¹⁹⁾ The aurone derivatives reported in this study appear superior to IMPY in pharmacokinetics, in addition to showing similar binding affinities sufficient for the imaging of A β plaques *in vivo*. The pharmacokinetics demonstrated by [¹²⁵I]45 are critical to the detection of A β plaques in the AD brain.

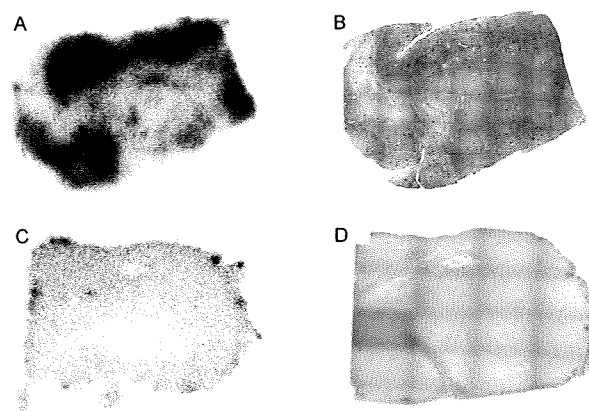


Fig. 16. *In Vitro* Autoradiography of [¹²⁵I]45 for Labeling of A β Plaques in AD Brain Sections

In vitro autoradiography of [¹²⁵I]45 reveals a distinct labeling of A β plaques in AD brain sections (A). Under similar conditions, there is very little labeling of [¹²⁵I]45 in control brain section (C). The presence and localization of A β plaques in the sections were confirmed with immunohistochemical staining using a monoclonal A β antibody (B, D).

Next, [¹²⁵I]45 was investigated for its binding affinity for A β plaques using *in vitro* autoradiography in human AD brain sections (Fig. 16). Autoradiographic images of [¹²⁵I]45 showed high levels of radioactivity in the brain sections (Fig. 16A). Furthermore, we confirmed that the hot spots of [¹²⁵I]45 corresponded with those of *in vitro* immunohistochemical staining in the same brain sections (Fig. 16B). In contrast, normal human brain displayed no remarkable accumulation of [¹²⁵I]45 (Fig. 16C), correlating well with the absence of A β plaques (Fig. 16D). These results demonstrate the feasibility of using [¹²⁵I]45 as a probe for detecting A β plaques in the brains of AD patients with SPECT.

Conclusion

We successfully designed and synthesized several basic structures that can function as useful A β imaging probes. We hope that the A β imaging probes will contribute to improved diagnosis and accelerate the discovery of effective therapeutic agents for AD in the near future.

Acknowledgments All the results in this review were obtained at the University of Pennsylvania, Nagasaki University, and Kyoto University. I would like to express sincere appreciation to Professor Hank F. Kung, Professor Morio Nakayama, and Professor Hideo Saji for their helpful, continuous advice and support. The research reviewed in this paper was possible only through the dedication, enthusiasm, and creativity of all my coworkers, whose names are acknowledged in the publications from our laboratory cited here. These studies were supported by a Grant-in Aid for Young Scientists (A) and (B) from the Ministry of Education, Culture, Sports, Science and Technology, the Industrial Technology Research Grant Program from New Energy and Industrial Technology Development Organization (NEDO), the Program for Promotion of Fundamental Biomedical Innovation (NIBIO), and a Health Labour Sciences Research Grant.

References

- 1) Klunk W. E., *Neurobiol. Aging*, **19**, 145–147 (1998).
- 2) Selkoe D. J., *Physiol. Rev.*, **81**, 741–766 (2001).
- 3) Mathis C. A., Wang Y., Klunk W. E., *Curr. Pharm. Des.*, **10**, 1469–1492 (2004).
- 4) Nordberg A., *Lancet Neurol.*, **3**, 519–527 (2004).
- 5) Mathis C. A., Wang Y., Holt D. P., Huang G. F., Debnath M. L., Klunk W. E., *J. Med. Chem.*, **46**, 2740–2754 (2003).
- 6) Klunk W. E., Engler H., Nordberg A., Wang Y., Blomqvist G., Holt D. P., Bergstrom M., Savitcheva I., Huang G. F., Estrada S., Aussen B.,

- Debnath M. L., Barletta J., Price J. C., Sandell J., Lopresti B. J., Wall A., Koivisto P., Antoni G., Mathis C. A., Langstrom B., *Ann. Neurol.*, **55**, 306—319 (2004).
- 7) Klunk W. E., Mathis C. A., Price J. C., Lopresti B. J., DeKosky S. T., *Brain*, **129**, 2805—2807 (2006).
 - 8) Rowe C. C., Ng S., Ackermann U., Gong S. J., Pike K., Savage G., Cowie T. F., Dickinson K. L., Maruff P., Darby D., Smith C., Woodward M., Merory J., Tochon-Danguy H., O'Keefe G., Klunk W. E., Mathis C. A., Price J. C., Masters C. L., Villemagne V. L., *Neurology*, **68**, 1718—1725 (2007).
 - 9) Ono M., Wilson A., Nobrega J., Westaway D., Verhoeff P., Zhuang Z. P., Kung M. P., Kung H. F., *Nucl. Med. Biol.*, **30**, 565—571 (2003).
 - 10) Verhoeff N. P., Wilson A. A., Takeshita S., Trop L., Hussey D., Singh K., Kung H. F., Kung M. P., Houle S., *Am. J. Geriatr. Psychiatry*, **12**, 584—595 (2004).
 - 11) Rowe C. C., Ackerman U., Browne W., Mulligan R., Pike K. L., O'Keefe G., Tochon-Danguy H., Chan G., Berlangieri S. U., Jones G., Dickinson-Rowe K. L., Kung H. P., Zhang W., Kung M. P., Skovronsky D., Dyrks T., Holl G., Krause S., Friebe M., Lehman L., Lindemann S., Dinkelborg L. M., Masters C. L., Villemagne V. L., *Lancet Neurol.*, **7**, 129—135 (2008).
 - 12) Zhang W., Oya S., Kung M. P., Hou C., Maier D. L., Kung H. F., *Nucl. Med. Biol.*, **32**, 799—809 (2005).
 - 13) Kudo Y., Okamura N., Furumoto S., Tashiro M., Furukawa K., Maruyama M., Itoh M., Iwata R., Yanai K., Arai H., *J. Nucl. Med.*, **48**, 553—561 (2007).
 - 14) Agdeppa E. D., Kepe V., Liu J., Flores-Torres S., Satyamurthy N., Petric A., Cole G. M., Small G. W., Huang S. C., Barrio J. R., *J. Neurosci.*, **21**, RC189 (2001).
 - 15) Shoghi-Jadid K., Small G. W., Agdeppa E. D., Kepe V., Ercoli L. M., Siddarth P., Read S., Satyamurthy N., Petric A., Huang S. C., Barrio J. R., *Am. J. Geriatr. Psychiatry*, **10**, 24—35 (2002).
 - 16) Small G. W., Kepe V., Ercoli L. M., Siddarth P., Bookheimer S. Y., Miller K. J., Lavretsky H., Burggren A. C., Cole G. M., Vinters H. V., Thompson P. M., Huang S. C., Satyamurthy N., Phelps M. E., Barrio J. R., *N. Engl. J. Med.*, **355**, 2652—2663 (2006).
 - 17) Braskie M. N., Klunder A. D., Hayashi K. M., Protas H., Kepe V., Miller K. J., Huang S. C., Barrio J. R., Ercoli L. M., Siddarth P., Satyamurthy N., Liu J., Toga A. W., Bookheimer S. Y., Small G. W., Thompson P. M., *Neurobiol. Aging*, in press.
 - 18) Kung M. P., Hou C., Zhuang Z. P., Zhang B., Skovronsky D., Trojanowski J. Q., Lee V. M., Kung H. F., *Brain Res.*, **956**, 202—210 (2002).
 - 19) Zhuang Z. P., Kung M. P., Wilson A., Lee C. W., Plossl K., Hou C., Holtzman D. M., Kung H. F., *J. Med. Chem.*, **46**, 237—243 (2003).
 - 20) Kung M. P., Hou C., Zhuang Z. P., Cross A. J., Maier D. L., Kung H. F., *Eur. J. Nucl. Med. Mol. Imaging*, **31**, 1136—1145 (2004).
 - 21) Newberg A. B., Wintering N. A., Plossl K., Hochold J., Stabin M. G., Watson M., Skovronsky D., Clark C. M., Kung M. P., Kung H. F., *J. Nucl. Med.*, **47**, 748—754 (2006).
 - 22) Kung H. F., Lee C. W., Zhuang Z. P., Kung M. P., Hou C., Plossl K., *J. Am. Chem. Soc.*, **123**, 12740—12741 (2001).
 - 23) Chishti M. A., Yang D. S., Janus C., Phinney A. L., Horne P., Pearson J., Strome R., Zuker N., Loukides J., French J., Turner S., Lozza G., Grilli M., Kunicki S., Morissette C., Paquette J., Gervais F., Bergeron C., Fraser P. E., Carlson G. A., George-Hyslop P. S., Westaway D., *J. Biol. Chem.*, **276**, 21562—21570 (2001).
 - 24) Janus C., Chishti M. A., Westaway D., *Biochim. Biophys. Acta*, **1502**, 63—75 (2000).
 - 25) Ono M., Kawashima H., Nonaka A., Kawai T., Haratake M., Mori H., Kung M. P., Kung H. F., Saji H., Nakayama M., *J. Med. Chem.*, **49**, 2725—2730 (2006).
 - 26) Ono M., Kung M. P., Hou C., Kung H. F., *Nucl. Med. Biol.*, **29**, 633—642 (2002).
 - 27) Gomez-Isla T., Price J. L., McKeel D. W., Jr., Morris J. C., Growdon J. H., Hyman B. T., *J. Neurosci.*, **16**, 4491—4500 (1996).
 - 28) Haroutunian V., Perl D. P., Purohit D. P., Marin D., Khan K., Lantz M., Davis K. L., Mohs R. C., *Arch. Neurol.*, **55**, 1185—1191 (1998).
 - 29) Price J. L., Morris J. C., *Ann. Neurol.*, **45**, 358—368 (1999).
 - 30) Styren S. D., Hamilton R. L., Styren G. C., Klunk W. E., *J. Histochem. Cytochem.*, **48**, 1223—1232 (2000).
 - 31) Dishino D. D., Welch M. J., Kilbourn M. R., Raichle M. E., *J. Nucl. Med.*, **24**, 1030—1038 (1983).
 - 32) Price J. C., Klunk W. E., Lopresti B. J., Lu X., Hoge J. A., Ziolkowski S. K., Holt D. P., Meltzer C. C., DeKosky S. T., Mathis C. A., *J. Cereb. Blood Flow Metab.*, **25**, 1528—1547 (2005).
 - 33) Lopresti B. J., Klunk W. E., Mathis C. A., Hoge J. A., Ziolkowski S. K., Lu X., Meltzer C. C., Schimmel K., Tsopelas N. D., DeKosky S. T., Price J. C., *J. Nucl. Med.*, **46**, 1959—1972 (2005).
 - 34) Wang Y., Klunk W. E., Huang G. F., Debnath M. L., Holt D. P., Mathis C. A., *J. Mol. Neurosci.*, **19**, 11—16 (2002).
 - 35) Ono K., Yoshiike Y., Takashima A., Hasegawa K., Naiki H., Yamada M., *J. Neurochem.*, **87**, 172—181 (2003).
 - 36) Zhuang Z. P., Kung M. P., Hou C., Skovronsky D. M., Gur T. L., Plossl K., Trojanowski J. Q., Lee V. M., Kung H. F., *J. Med. Chem.*, **44**, 1905—1914 (2001).
 - 37) Ono M., Yoshida N., Ishibashi K., Haratake M., Arano Y., Mori H., Nakayama M., *J. Med. Chem.*, **48**, 7253—7260 (2005).
 - 38) Espeseth A. S., Xu M., Huang Q., Coburn C. A., Jones K. L., Ferrer M., Zuck P. D., Strulovici B., Price E. A., Wu G., Wolfe A. L., Lineberger J. E., Sardana M., Tugusheva K., Pietrak B. L., Crouthamel M. C., Lai M. T., Dodson E. C., Bazzo R., Shi X. P., Simon A. J., Li Y., Hazuda D. J., *J. Biol. Chem.*, **280**, 17792—17797 (2005).
 - 39) Iwatsubo T., Odaka A., Suzuki N., Mizusawa H., Nukina N., Ihara Y., *Neuron*, **13**, 45—53 (1994).
 - 40) Morris J. C., Storandt M., McKeel D. W. Jr., Rubin E. H., Price J. L., Grant E. A., Berg L., *Neurology*, **46**, 707—719 (1996).
 - 41) Zhuang Z. P., Kung M. P., Hou C., Plossl K., Skovronsky D., Gur T. L., Trojanowski J. Q., Lee V. M., Kung H. F., *Nucl. Med. Biol.*, **28**, 887—894 (2001).
 - 42) Ono M., Haratake M., Mori H., Nakayama M., *Bioorg. Med. Chem.*, **15**, 6802—6809 (2007).
 - 43) Ono M., Hori M., Haratake M., Tomiyama T., Mori H., Nakayama M., *Bioorg. Med. Chem.*, **15**, 6388—6396 (2007).
 - 44) Ono K., Hasegawa K., Naiki H., Yamada M., *J. Neurosci. Res.*, **75**, 742—750 (2004).
 - 45) Yang F., Lim G. P., Begum A. N., Ubeda O. J., Simmons M. R., Ambegaokar S. S., Chen P. P., Kaye R., Glabe C. G., Frautschy S. A., Cole G. M., *J. Biol. Chem.*, **280**, 5892—5901 (2005).
 - 46) Ryu E. K., Choe Y. S., Lee K. H., Choi Y., Kim B. T., *J. Med. Chem.*, **49**, 6111—6119 (2006).
 - 47) Ono M., Maya Y., Haratake M., Ito K., Mori H., Nakayama M., *Biochem. Biophys. Res. Commun.*, **361**, 116—121 (2007).
 - 48) Maya Y., Ono M., Watanabe H., Haratake M., Saji H., Nakayama M., *Bioconjug. Chem.*, **20**, 95—101 (2009).
 - 49) Roberts M. J., Bentley M. D., Harris J. M., *Adv. Drug. Deliv. Rev.*, **54**, 459—476 (2002).
 - 50) Harris J. M., Chess R. B., *Nat. Rev. Drug. Discov.*, **2**, 214—221 (2003).
 - 51) Kung M. P., Hou C., Zhuang Z. P., Skovronsky D., Kung H. F., *Brain Res.*, **1025**, 98—105 (2004).
 - 52) Zhang W., Oya S., Kung M. P., Hou C., Maier D. L., Kung H. F., *J. Med. Chem.*, **48**, 5980—5988 (2005).

